$\times 10^7$ M^{-1} s^{-1} compared with 1×10^7 M^{-1} s^{-1} evaluated by Brown and co-workers.[22]

The application of the same procedure to $Mn(CO)_5^-$ failed to produce reproducible results owing to the large corrections for the charging current and ohmic drop at the requisite fast scan rates in Table I. An approximate value of k_2 was obtained from the relationship $k_2 = n\mathcal{F}v/(C_0^*RT)$ when $i_c/i_a \cong 1$, as also derived by Nicholson and co-workers.[27] For $Mn(CO)_5^-$, this current ratio was attained at $v \simeq 175\,000$, from which $k_2 = 7 \times 10^8$ M^{-1} s^{-1}, in reasonable agreement with a value of $k_2 = 9 \times 10^8$ M^{-1} s^{-1} evaluated by Brown and co-workers.[22] The validity of this relationship is supported by the value of $k_2 = 1.5 \times 10^7$ M^{-1} s^{-1} for $Mn(CO)_4PPh_3^-$ obtained at $v = 4000$ for $i_c/i_a = 1.0$ (vide supra).

Acknowledgment. We thank the National Science Foundation and the R. A. Welch Foundation for financial support.

Registry No. I, 47902-58-9; I·AsF_6^-, 117872-92-1; II, 115162-69-1; $Mn(CO)_5^-$, 14971-26-7; $Mn(CO)_4PPh_3^-$, 53418-18-1; $Mn(CO)_2(\eta^2\text{-DPPE})_2^\bullet$, 118490-97-4; $Mn(CO)_2(\eta^2\text{-DPPE})(\eta^1\text{-DPPE})^\bullet$, 115162-72-6; $Mn(CO)_3(Ph_3P)_2^-$, 68033-53-4; $Mn(CO_3)(DPPE)^-$, 113821-86-6; $Mn(CO_3)((PhO)_3P)_2^-$, 68033-46-5; $Mn(CO_3)((o\text{-}CH_3C_6H_4O)_3P)_2^-$, 84180-09-6; $Mn(CO_3)((n\text{-}Bu_3)P)_2^-$, 113821-87-7; $Mn(CO_3)((i\text{-}PrO)_3P)_2^-$, 113890-85-0; $Mn(CO_3)((i\text{-}Pr)_3P)_2^-$, 113821-88-8; $Mn(CO_6)^+BF_4^-$, 15557-71-8; $Mn(CO)_5PPh_3^+BF_4^-$, 54039-46-2; $Mn(CO)_3(NCCH_3)_3^+BF_4^-$, 68928-06-3; *trans*-$Mn(CO)_2(DPPE)_2^+PF_6^-$, 34216-61-0; *cis*-$Mn(CO)_2(CNCH_3)_4^+PF_6^-$, 65546-42-1; $Mn(CNC_6H_4CH_3)_6^+PF_6^-$, 118419-41-3; *cis*-$Mn(CO)_2[P(OMe)_3]_4^+BF_4^-$, 118419-39-9; $Mn(CO)_5^\bullet$, 14971-26-7; $Mn(CO)_3(PPh_3)_2^\bullet$, 27903-25-9; $Mn(CO)_4PPh_3^\bullet$, 14971-47-2; $Mn(CO)_3[P(OPh)_3]_2^\bullet$, 113821-89-9; *trans*-$Mn(CO)_2(DPPE)_2^+$, 47902-56-7; Pt, 7440-06-4; carbon monoxide, 630-08-0; tetra-*n*-butylammonium hexafluorophosphate, 3109-63-5.

Contribution from the Department of Chemistry, University of Tennessee, Knoxville, Tennessee 37996, and Savannah River Laboratory, E. I. du Pont de Nemours & Company, Inc., Aiken, South Carolina 29808

Electrocatalytic Reduction of Nitrate in Sodium Hydroxide Solution in the Presence of Low-Valent Cobalt-Cyclam Species

Hu-Lin Li,[†,‡] William C. Anderson,[†] James Q. Chambers,*[,†] and David T. Hobbs[§]

Received August 26, 1988

In concentrated NaOH solution nitrate and nitrite ions are efficiently reduced to a mixture of products including hydroxylamine and ammonia via an electrocatalytic process in the presence of cobalt complexes of 1,4,8,11-tetraazacyclotetradecane (cyclam). A key mechanistic role is proposed for Co^I(cyclam)NO_3, which is generated in the diffusion layer at ca. −1.3 V vs SCE. The lack of dependence on pH of either the catalytic peak potential or the peak current indicates that metal hydride intermediate species are not involved in the initial steps of the reduction process. Both Co^I and Co^{III} intermediates in the nitrate reduction are detected in collection experiments with a gold ring–disk electrode.

Transition-metal macrocyclic amine complexes based on ligands such as 1,4,8,11-tetraazacyclotetradecane have the property of catalyzing a variety of redox processes of a remarkable diversity.[1-6] Electrocatalytic reductions of dioxygen,[3] carbon dioxide,[1,2,4] the N–O bond in nitrate and nitrite,[6] and carbon–halogen bonds[5] have been reported. Schemes suggested to explain the electrocatalytic activity of the these species generally invoke the chemical stability imparted to the lower oxidation states by the macrocylic ligand and the chemistry made possible by the availability of the labile axial coordination sites.

Of particular interest to us were the reports by Taniguchi et al.[6] that metal cyclam complexes, specifically the classical 14-membered 1,4,8,11-tetraazacyclotetradecane macrocycle complexes of cobalt and nickel, act as excellent catalysts for the reduction of nitrate and nitrite in aqueous solutions. As part of a project involving the destruction of nitrate in nuclear waste solutions, the reduction of nitrate and nitrite in concentrated sodium hydroxide solutions has been under study in our laboratories for some time.[7,8] At several metal and phthalocyanine-coated electrodes nitrate and nitrite ions are reduced to mixtures of products that include dinitrogen, hydroxylamine, and ammonia. These electrode reactions, which are not diffusion-limited, give rise to voltammetric currents that increase exponentially at the foot of the hydrogen discharge process. The present study was undertaken to determine the compatibility of the metal–cyclam electrocatalyzed cycle for the reduction of nitrate under the strongly alkaline conditions that are encountered in the treatment of nuclear waste solutions. Several details regarding the role of reduced Co(cyclam) species in the mechanism of the nitrate reduction have been revealed in the course of the study.

Experimental Section

Chemicals. Reagent grade chemicals and doubly distilled water that had been passed through a Millipore purification column were used to prepare all solutions. The [*trans*-Cl_2Co^{III}(cyclam)]Cl complex, where cyclam is 1,4,8,11-tetraazacyclotetradecane (Aldrich), was prepared by literature procedures.[9] Ferrozine, 3-(2-pyridyl)-5,6-diphenyl-1,2,4-triazine-4,4′-disulfonic acid, was obtained from Fluka. The deuterated reagents NaOD and D_2O were obtained from the Cambridge Isotope Laboratory.

Electrodes and Cells. The working electrodes for voltammetry were disk electrodes constructed from lead rod (Aldrich, 99.9995%), gold wire (Aldrich, 99.99%), silver wire (GR), and a mercury surface prepared by electroplating a gold disk; the geometrical areas for the electrodes were 0.126, 0.0314, 0.002, and 0.0113 cm^2, respectively. Larger area electrodes were used for the controlled-potential electrolyses. A large area nickel plate was used for the counter electrode. A SCE was the reference electrode in all experiments. The rotating gold ring–gold disk electrode (Pine Instrument Co., Model AFDT27) had dimensions of $r_1 = 0.250$ cm, $r_2 = 0.2705$ cm, and $r_3 = 0.3325$ cm.

Simple glass cells with provision for oxygen removal by flushing with argon were employed. "High-purity" argon was purified further by passage through a 3-ft column containing Mn(II) dispersed on vermiculite.[10]

Instrumentation. Electrochemical experiments were carried out by using a Bioanalytical Systems electrochemical analyzer, Model BAS-100.

[†] University of Tennessee.
[‡] Present address: Department of Chemistry, Lanzhou University, Ganzu, China.
[§] E. I. du Pont de Nemours & Co., Inc.

(1) Fisher, B.; Eisenberg, R. *J. Am. Chem. Soc.* **1980**, *102*, 7361.
(2) Beley, M.; Collin, J.-P.; Ruppert, R.; Sauvage, J.-P. *J. Am. Chem. Soc.* **1986**, *108*, 7461.
(3) Geiger, T.; Anson, F. C. *J. Am. Chem. Soc.* **1981**, *103*, 7489.
(4) Bradley, M. G.; Tysak, T.; Graves, D. J.; Vlachopoulos, N. A. *J. Chem. Soc., Chem. Commun.* **1983**, 349.
(5) (a) Becker, J. Y.; Kerr, J. B.; Pletcher, D.; Rosas, R. *J. Electroanal. Chem. Interfacial Electrochem.* **1981**, *117*, 87. (b) Gosden, C.; Kerr, J. B.; Pletcher, D.; Rosas, R. *Ibid.* **1981**, *117*, 101.
(6) (a) Taniguchi, I.; Nakashima, N.; Yasukouchi, K. *J. Chem. Soc., Chem. Commun.* **1986**, 1814. (b) Taniguchi, I.; Nakashima, N.; Matsushita, K.; Yasukouchi, K. *J. Electroanal. Chem. Interfacial Electrochem.* **1987**, *224*, 199.
(7) Li, H.-L.; Robertson, D. H.; Chambers, J. Q.; Hobbs, D. T. *J. Electrochem. Soc.* **1988**, *135*, 1154.
(8) Li, H.-L.; Chambers, J. Q.; Hobbs, D. T. *J. Appl. Electrochem.* **1988**, *18*, 454.
(9) Bosnich, B.; Poon, C. K.; Tobe, M. L. *Inorg. Chem.* **1965**, *4*, 1102.
(10) Brown, T. L.; Dickerhoot, C. W.; Bafus, D. A.; Morgan, G. L. *Rev. Sci. Instrum.* **1962**, *22*, 491.

0020-1669/89/1328-0863$01.50/0 © 1989 American Chemical Society

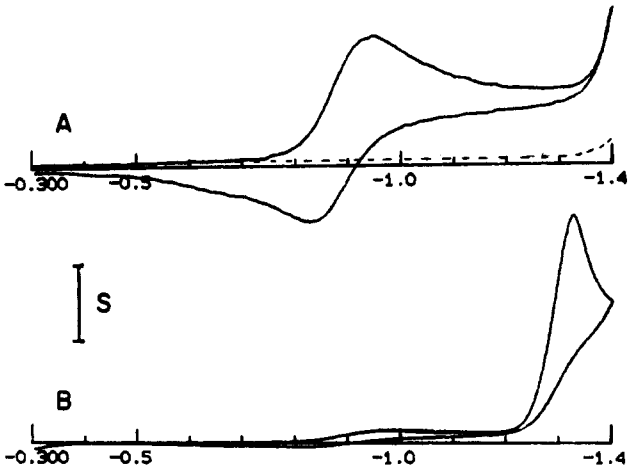

Figure 1. (A) Cyclic voltammogram of 2.0×10^{-3} M Co^{III}(cyclam) in 3.0 M NaOH at a Au(Hg) disk electrode. Conditions: sweep rate, 20 mV s^{-1}; $S = 2 \times 10^{-6}$ A; the dashed line is the current in the absence of the Co^{III}(cyclam) complex. (B) Cyclic voltammogram of the solution from part A with 3×10^{-3} M $NaNO_3$ added.

A Pine Instrument Co. bipotentiostat and rotators (Model Nos. RDE4 and PIR) were used for the ring–disk experiments. Ultraviolet/visible absorption spectra were obtained on a Cary Model 219 spectrophotometer.

Procedures. Analytical procedures have been described previously.[8] Nitrate and nitrite were determined by ion chromatography, ammonia was determined by Kjeldahl titration, and hydroxylamine was determined by the ferrozine colorimetric procedure of Dias et al.[11]

Results

Characterization of Co^{III}(cyclam) in Base. Although the 14-membered cyclic amine macrocyclic ligand and its metal complexes have been well studied, the literature is rather sketchy on the behavior of the Co(III) complex in strong base. Accordingly, cyclic voltammograms and visible absorption spectra of solutions of $[Co^{III}(cyclam)Cl_2]^+$ were obtained as a function of added standard NaOH solution. The results show that the quasi-reversible $Co^{III/II}$(cyclam) couple is strongly pH-dependent and moderately complex.

Addition of small amounts of NaOH to the emerald green solutions of the *trans*-dichlorocyclamcobalt(III) complex (λ_{max} = 433, 633 nm; c.f. 440, 640 nm[9]) causes marked changes in the visible absorption spectrum. Up to less than 1 equiv of base, isosbestic points are seen at 429 and 609 nm. The isosbestic points are lost as more base is added, indicating the existence of more than two species in equilibrium, and at 2 equiv, the spectrum becomes independent of base up to 3 M NaOH. This behavior is consistent with the known rapid base-catalyzed hydrolysis of the *trans*-dichloro complex[12] and formation of the *trans*-dihydroxo complex. The absorption spectrum of the solution exhibits maxima at 387 nm (a = 59.9 M^{-1} cm^{-1}) and 540 nm (a = 49.0 M^{-1} cm^{-1}) and is assigned to species **1**. The shift of λ_{max} to a lower value

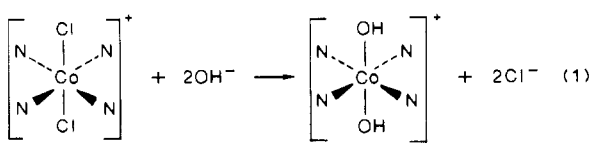

(1)

1

is consistent with formation of the dihydroxy complex according to the spectrochemical series.[13] Beer's law is obeyed up to a concentration of 0.015 M. Neutralization of the solution with $HClO_4$ produces a pale green solution that has an absorption spectrum which matches the reported spectrum[3] of the known *trans*-Co^{III}(cyclam)$(H_2O)_2^{3+}$ species.

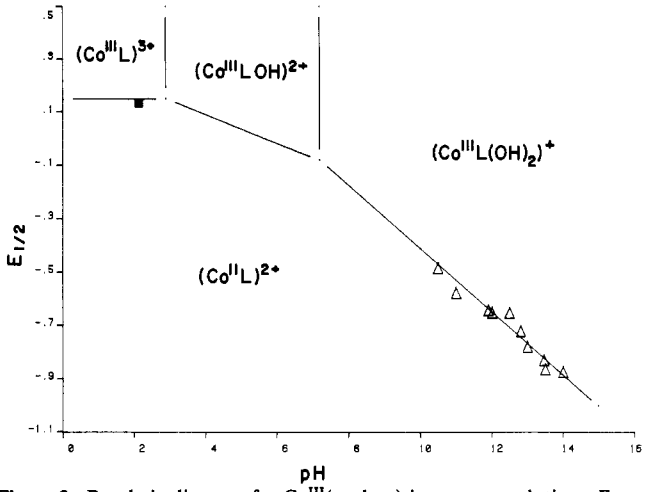

Figure 2. Pourbaix diagram for Co^{III}(cyclam) in aqueous solution. $E_{1/2} = (E_p^a + E_p^c)/2$ in V vs SCE; L = cyclam.

The cyclic voltammetry of the Co^{III}(cyclam) complex in base is more intricate than suggested by the spectrophotometric titrations. In Figure 1 is shown the quasi-reversible slow-sweep-rate cyclic voltammogram of **1** in 3 M NaOH. Identical voltammograms were obtained when the *trans*-Cl_2Co^{III}(cyclam) complex was either added directly to the NaOH solution or when the chloride ligands were exchanged prior to the addition of the base by passage of the complex through an anion-exchange column in the hydroxide form. Similar voltammograms were obtained at mercury, gold, lead, and silver electrodes, although the degree of reversibility was dependent on the electrode material to a certain extent.

In spite of careful attention to the removal of oxygen and preelectrolysis of the solution, Coulometric analysis gave variable n values. Electrolysis at a gold foil electrode at −1.1 V gave n = 0.9, while electrolysis at a mercury pool electrode gave n = 1.3. Reverse coulometry regenerated only a fraction of the Co^{III}(cyclam) complex. Slow disproportionation of Co^{II}(cyclam) in base and reaction of Co^{I}(cyclam) with solvent could account for this behavior.

The anodic segment of the voltammogram of Figure 1 indicates a two-step process, which becomes more evident at faster sweep rates. The peak current ratio, i_p^{anod}/i_p^{cath}, is significantly less than unity. This complex behavior becomes even more evident as the NaOH concentration is decreased by titration with concentrated $HClO_4$. Both the shape and the position of the $Co^{III/II}$(cyclam) voltammetric wave are markedly dependent on the solution pH in contrast to the absorption spectra of the Co^{III}(cyclam) complex, which were independent of the solution pH in the presence of excess base. The wave shifts in the positive direction as the solution is neutralized, and in the presence of excess $HClO_4$, the known[3] quasi-reversible *trans*-$(H_2O)_2Co(cyclam)^{3+/2+}$ couple appears.

Similar behavior is seen when a 0.1 M KCl solution of the *trans*-Cl_2Co^{III}(cyclam) complex is neutralized with concentrated NaOH solution. The quasi-reversible $Co^{III/II}$ wave, which appears at ca. −0.1 V vs SCE in agreement with Taniguchi et al.,[6] is converted into a drawn-out multistep process by the addition of base.

An approximate Pourbaix diagram for the $Co^{III/II}$ couple is shown in Figure 2 where the $E_{1/2}$ values have been estimated from the cyclic voltammograms obtained during the titrations with $HClO_4$ and NaOH. In the pH range from 10 to 14 we find $E_{1/2}$ = 0.69 − (0.113 ± 0.009)pH at room temperature. The uncertainty in these values is related to the low buffer capacity of the solutions near the equivalent points of the titrations and the poorly defined voltammetric waves. Nonetheless, the behavior is consistent with the known acid–base properties of the *trans*-$(H_2O)_2Co^{III}$(cyclam) complex: pK_1 = 2.9; pK_2 = 6.9.[14] These

(11) Dias, F.; Olojola, A. S.; Jaselskis, B. *Talanta* **1979**, *26*, 47.
(12) Poon, C. K.; Tobe, M. L. *J. Chem. Soc. A* **1967**, 2069.
(13) Cotton, F. A.; Wilkinson, G. *Advanced Inorganic Chemistry*, 4th ed.; Wiley-Interscience: New York, 1980; p 663.

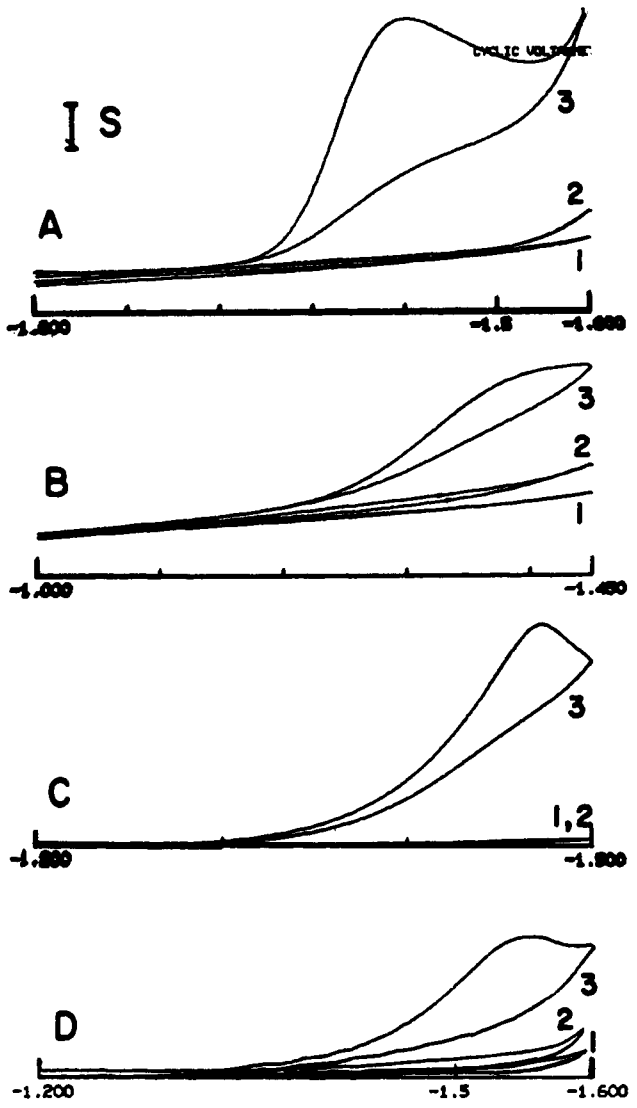

Figure 3. Cyclic voltammograms of (1) 3.0 M NaOH, (2) plus 0.012 M $NaNO_3$, (3) plus 1.14×10^{-4} M Co^{III}(cyclam) at (A–D) gold, silver, Au(Hg), and lead electrodes. Conditions: sweep rate, 20 mV s^{-1}; current scale (S) = 50×10^{-6} A (A–C), 500×10^{-6} A (D).

pK values and the known $E^{\circ\prime}$ of the *trans*-$(H_2O)_2Co^{III/II}$(cyclam) couple in $HClO_4$[3] were used to locate the boundaries, drawn with slopes of 0, 60, and 120 mV/pH unit, in the Pourbaix diagram of Figure 2. The solid point in Figure 2 is a measured value calculated from the nearly reversible cyclic voltammogram obtained in the presence of excess $HClO_4$. Although the complexities of the cyclic voltammetry strongly indicate that electrochemical square schemes are operative, which probably involve coupled proton transfer[15] or conformational[16] steps, the spectral and voltammetric data strongly indicate that the following overall electrode reaction takes place in NaOH solution.

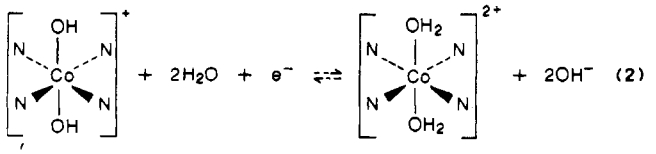

(14) Poon, C. K.; Tobe, M. L. *Inorg. Chem.* **1968**, *7*, 2398.
(15) Laviron, E. *J. Electroanal. Chem. Interfacial Electrochem.* **1983**, *146*, 1, 15; **1984**, *164*, 213; **1984**, *169*, 29.
(16) Evans, D. H.; O'Connell, K. M. In *Electroanalytical Chemistry*; Bard, A. J., Ed.; Marcel Dekker: New York, 1986; Vol. 14.

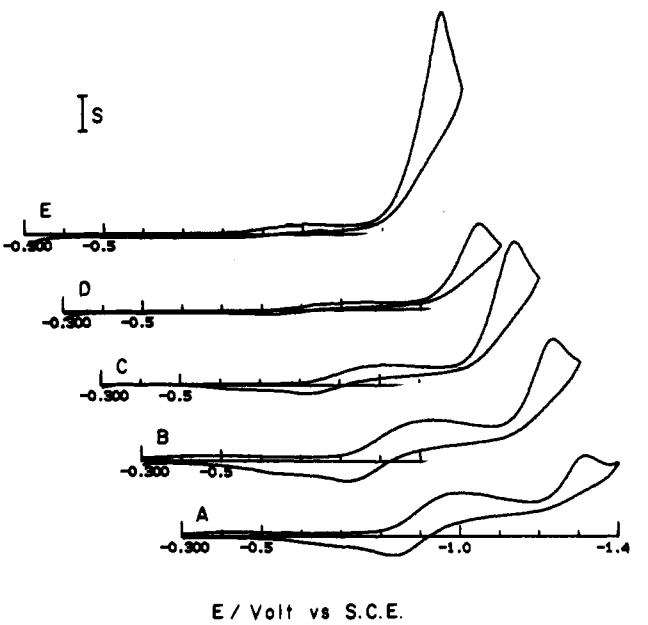

Figure 4. Cyclic voltammograms of (A–E) 0.1, 0.2, 0.4, 0.6, and 2.6×10^{-3} M $NaNO_2$ in 2.0×10^{-3} M Co^{III}(cyclam) and 3.0 M NaOH at a Au(Hg) disk electrode. Conditions: sweep rate, 20 mV s^{-1}; current scale = 1.0×10^{-6} A (A and B), 2.0×10^{-6} A (C), 5.0×10^{-6} A (D and E).

Cyclic Voltammetry of Co^{III}(cyclam)/Nitrate and Co^{III}(cyclam)/Nitrite Solutions. In agreement with the results of Taniguchi et al. in neutral solution,[6] the presence of the Co^{III}(cyclam) complex electrocatalyzes the irreversible reduction of either nitrate or nitrite ions in NaOH solution. This behavior is shown in Figure 1B by the appearance in the presence of nitrate of a large irreversible reduction wave, which is proportional to nitrate concentration, in the −1.3 to −1.4 V region. Representative cyclic voltammograms at gold, silver, mercury, and lead electrodes are shown in Figure 3. In the absence of the Co^{III}(cyclam) complex, addition of nitrate to the solution (curves 2 in Figure 3) results in an increase in the cathodic current due to the very slow reduction of nitrate. This brute force reduction of nitrate, which gives a mixture of products including nitrite, dinitrogen, hydroxylamine, and ammonia, has been studied previously at a variety of working electrodes.[7,8] In the presence of the Co^{III}(cyclam) complex (curves 3 in Figure 3), however, a diffusion-limited, irreversible peak voltammogram is seen at potentials positive of the cathodic limit for each electrode material examined. (In addition to those of Figure 3, nickel and platinum electrodes have been used.)

Very similar behavior is observed for the reduction of nitrite in the presence of the Co^{III}(cyclam) complex; see Figure 4. The peak currents for the reduction of either nitrate or nitrite are proportional to concentration over the range from 10^{-5} to 10^{-2} M.

As seen in Figures 3 and 4, the reduction of either nitrate or nitrite occurs in a potential region for all the cathode materials examined where there is no faradaic reaction for the Co^{III}(cyclam) complex in the absence of nitrate or nitrite. In Figure 3 the cathodic current for the reduction of the Co^{III}(cyclam) complex, present at a concentration of 1.14×10^{-4} M, is swamped by the much larger kinetic current for the reduction of nitrate. Significantly, when the complex is present at much higher concentrations, the addition of either nitrite or nitrate has a negligible effect on either the shape or the peak heights of the quasi-reversible $Co^{III/II}$(cyclam) couple at ca. −0.8 V vs SCE.

The peak voltammogram for the catalyzed reduction of nitrate is remarkably independent of solution pH. This was demonstrated at two concentrations of the catalyst. First, in parallel with the titration of the Co^{III}(cyclam) complex described above, cyclic voltammograms were obtained on solutions of 2.0 mM catalyst and 5.0 mM $NaNO_3$ in 0.1 M KCl at a Au(Hg) electrode as a function of added base. In 0.1 M KCl, in agreement with the results of Taniguchi et al.[6], a peak voltammogram with a peak voltammogram with a peak potential of −1.38 V vs SCE was observed (sweep rate = 20 mV s^{-1}). Both the peak current and

Table I. Controlled-Potential Electrolysis of 4.0 mmol of $NaNO_3$ in 40 mL of 3.0 M NaOH Solution at Different Electrodes

cathode material	E_{appl}, V vs SCE	$[Co^{III}(cyclam)]$, μM	mmol of nitrate reduced	mmol of products			current efficiency, %
				NH_3	NO_2^-	NH_2OH	
Hg pool	−1.5	36	1.9	0.1	0.9	0.9	104
		0	0.4	0.1	0.2	0.2	39
nickel	−1.3	76	3.3	2.9	nd[a]	tr[b]	76
		0	0.4	0.2	0.2	nd	95
zinc	−1.5	76	4.0	3.4	nd	tr	120
		0	4.0	2.5	1.2	tr	116
lead	−1.6	76	3.8	3.4	nd	tr	97
		0	3.0	2.3	nd	nd	84
gold	−1.6	38	2.6	0.8	1.1	0.7	40
		0	0.6	nd	0.3	0.3	47
silver	−1.5	76	1.4	1.1	0.1	nd	61
		0	0.5	0.1	0.2	0.2	32

[a] Not detected. [b] Trace detected.

Table II. Controlled-Potential Electrolysis of 4.0 mmol of $NaNO_2$ in 40 mL of 3.0 M NaOH Solution at Different Electrodes

cathode material	E_{appl}, V vs SCE	$[Co^{III}(cyclam)]$, μM	mmol of nitrite reduced	mmol of products		current efficiency, %
				NH_3	NH_2OH	
Hg pool	−1.5	38	3.0	0.2	2.2	81
		0	0.1	nd[a]	0.1	69
nickel	−1.3	76	3.8	1.5	tr[b]	89
		0	0.5	0.3	nd	83
zinc	−1.5	76	3.9	3.0	0.9	96
		0	3.5	2.6	0.7	93
lead	−1.6	76	3.6	2.7	0.8	100
		0	0.2	0.1	0.1	21
gold	−1.6	38	3.1	1.9	1.2	77
		0	1.0	0.7	0.3	98

[a] Not detected. [b] Trace detected.

peak potential for this wave were independent of added NaOH. At a lower concentration of the Co^{III}(cyclam) complex, 2×10^{-5} M, the peak current and potential were invarient from 0.2 to 3.0 M NaOH.

The independence of the nitrate reduction current and potential on pH is also further evidence that the *trans*-$(H_2O)_2Co^{II}$(cyclam) species is the thermodynamically stable product of the electrode reaction at −0.8 to −0.9 V. Thus it is this species that is present in the diffusion layer at potentials where the reduction of nitrate and nitrite takes place.

In the concentrated NaOH solutions the nitrate reduction peak currents exhibited a diffusion sweep rate dependence over the sweep rate range from 5 to 1000 mV s^{-1}; i.e. i_p = (sweep rate)$^{0.43}$. The peak potential, which was strongly dependent on the sweep rate, decreased ca. 60 mV/decade increase in sweep rate and merged into the background process at faster sweep rates.

Several experiments were carried out by using D_2O as the solvent with added NaOD; see Figure 5. At low sweep rates there is no significant difference between the cyclic voltammograms of the nitrate reduction process in H_2O and in D_2O. The peak voltammograms obtained at the faster sweep rates in D_2O, however, were more drawn out and moved into the background process at lower sweep rates than in H_2O. Interestingly, the cyclic voltammograms of the Co^{III}(cyclam) complex displays the two-step nature of the electrode process more clearly in D_2O than in H_2O. This is seen in Figure 5 where the anodic segment shows two obvious peak currents.

Controlled-Potential Electrolysis. Tables I and II give some results of controlled potential electrolysis of $NaNO_3$ and $NaNO_2$ solutions in 3 M NaOH in the presence and absence of the Co^{III}(cyclam) complex. All electrolyses were carried out at room temperature on solutions containing 4.0 mmol of substrate and were terminated after 3 h. Although all of the working electrodes had approximately the same area (5 cm^2), comparisons between different electrode materials based on these data should be regarded as qualitative since cell conditions (electrode geometry, stirring rates, etc.) were not uniform, and the electrolyses were not carried out to the same percent completion.

There are some points to be noted in the tables nonetheless. With the exception of the zinc cathode, which participates in a

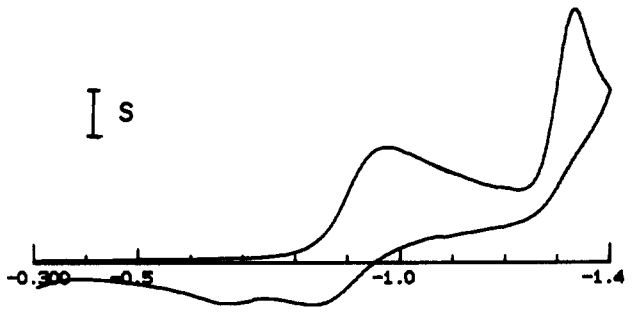

Figure 5. Cyclic voltammogram of 2.2×10^{-4} M $NaNO_3$, 2×10^{-3} M Co^{III}(cyclam), and 3.0 M NaOD in D_2O at a Au(Hg) disk electrode. Conditions: sweep rate, 20 mV s^{-1}; current scale (S), 1×10^{-6} A.

nonelectrochemical reductive pathway, addition of the Co^{III}(cyclam) complex significantly increases the amount of nitrate or nitrite reduced at potentials positive of the background discharge process. Within the experimental errors of the analytical procedures, there is a reasonable correspondence between the amount of nitrate (or nitrite) reduced and the amount of ammonia, hydroxylamine, and nitrite produced. The current efficiencies given in the tables were calculated by assuming that dinitrogen was formed to satisfy the mass balance. Dinitrogen is a likely product and has been unequivocally identified as an electrolysis product at nickel cathodes in the absence of the Co^{III}(cyclam) complex by mass spectroscopy.[7] Loss of gaseous ammonia is also a possibility. The low current efficiencies observed in several of the electrolyses are presumably due to the coevolution of hydrogen at the negative potentials employed. Finally, as noted previously,[8] the data suggest that a lead cathode is especially well suited for the reduction of nitrate and nitrite ions under these conditions. Accordingly, the combination of a lead cathode and a nickel anode for the oxidation of OH^- to O_2/or NH_2OH to N_2 would seem to be a good choice for the electrochemical destruction of nitrate and nitrite.

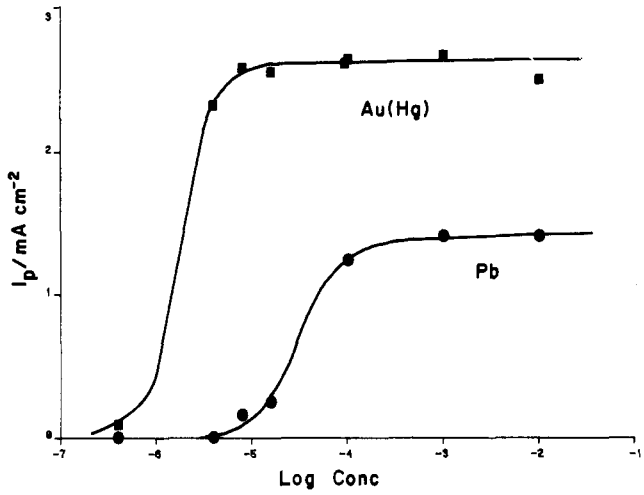

Figure 6. Variation of the catalytic peak current (mA/cm^2) for the reduction of nitrate in 3.0 M NaOH with concentration of Co^{III}(cyclam) at Au(Hg) and Pb electrodes.

Dependence on the Co^{III}(cyclam) Concentration. Both the peak current and the peak potentials of the nitrate reduction waves were dependent on the concentration of the Co^{III}(cyclam) complex. Above a given concentration level, which was dependent on the electrode material, the peak current was invarient with the concentration of the complex. This behavior is shown in Figure 6 for Au(Hg) and Pb electrodes. Similar behavior was seen at silver and bare gold electrodes. The peak potential of the wave shifted to more positive potentials as the Co^{III}(cyclam) concentration was increased. The variation was ca. 30 mV/decade increase in the concentration for the Au(Hg) and Pb cathodes used in the experiments of Figure 6.

Rotating Ring–Disk Experiments. A striking feature of the cyclic voltammograms of the nitrate (or nitrite) containing solutions in the presence of the Co^{III}(cyclam) complex is the location of the nitrate reduction wave on the potential axis. The wave appears in a region where the Co(cyclam) species, e.g. Co^{II}(cyclam)$^{2+}$, seem to be electroinactive in the absence of nitrate or nitrite ions. This behavior suggests that there is an interaction of a Co^{I} species with nitrate, i.e. either complexation of nitrate or rapid electron transfer to nitrate in the diffusion layer, which shifts the $Co^{II/I}$ redox couple to positive potentials out of the solvent discharge region.

In order to examine further whether the Co^{II}(cyclam) complex undergoes a faradaic process in the presence of nitrate, several rotating ring–disk experiments were performed with a Au disk–Au ring electrode. Since a ring–disk electrode allows independent control of the sensing ring electrode, the detection of an intermediate in an electrode process that is electroactive at potential of the disk electrode is possible. Detection of electroactive intermediates by fast-sweep cyclic voltammetry is less direct and often more difficult since it is necessary to monitor a faradaic current for the intermediate at some potential well removed from the potential where it is generated.

Figures 7 and 8 show the results of experiments where the ring current at −1.0 V was monitored as a function of the disk potential for different concentrations of the Co^{II}(cyclam) complex. As the disk potential is swept through the −0.8 to −0.9 V region, the ring current for the $Co^{III/II}$ reduction process decreases due to a shielding effect. This results because the flux of Co(III) to the ring is decreased by the disk electrode reaction (eq 2). After correction for background current, the shielding factor was in agreement with theory.[17] In the absence of added nitrate, the ring current exhibits some fluctuation at very negative potentials (ca. −1.5 V vs SCE) where gas evolution was evident at the disk. Significantly, in the presence of 5×10^{-3} M $NaNO_3$, when the disk potential reaches the region where the reduction of nitrate

(17) Napp, D. T.; Johnson, D. C.; Bruckenstein, S. *Anal. Chem.* **1967**, *39*, 481.

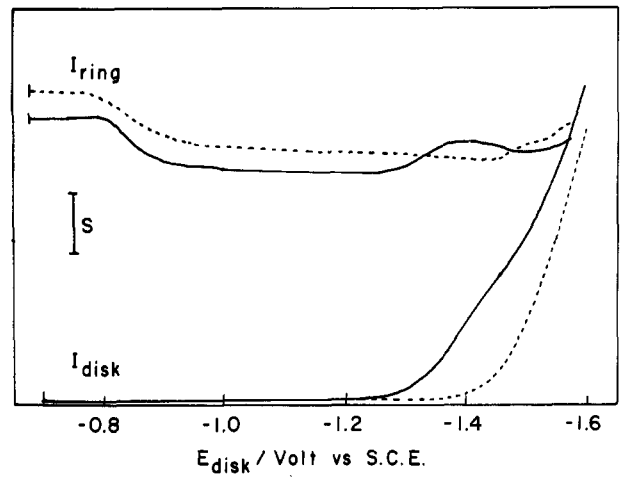

Figure 7. Rotating ring–disk voltammograms of 0.5×10^{-3} M Co^{III}(cyclam) and 1.0 M NaOH (dashed line), plus 5.0×10^{-3} M $NaNO_3$ (solid line). Conditions: rotation velocity, 1000 rpm; current scale, S = 0.2 mA (disk), 0.01 mA (ring); E_{ring}, −1.0 V vs SCE.

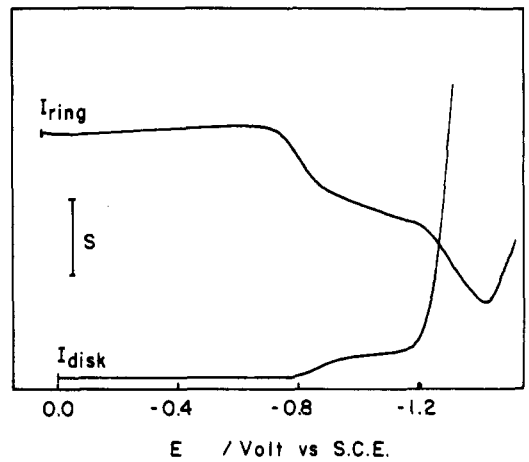

Figure 8. Rotating ring–disk voltammograms of 5.0×10^{-3} M Co^{III}(cyclam), 0.02 M $NaNO_3$, and 1.0 M NaOH. Conditions: rotation velocity, 1600 rpm; current scale, S = 1.0 mA (disk), 0.05 mA (ring); E_{ring} = −1.0 V vs SCE.

takes place, ca. −1.3 V, the cathodic ring current increases as shown in Figure 7 for the lower catalyst concentration. This current change is in the opposite direction expected for a simple redox process for which the ring collection current would become more anodic when reduction products were formed at the disk. A possible explanation for this behavior is that the flux of Co(III) to the ring is increased by the catalytic process for the reduction of nitrate. A scheme consistent with this idea is proposed below.

The magnitude of the ring current in the collection experiments of the type shown in Figure 7 was dependent on the concentration ratio of nitrate to cobalt. At a lower concentration of nitrate, or at a higher Co(cyclam) concentration, the collection current became more *anodic* when the disk potential was swept through the nitrate reduction process as seen in Figure 8. This is consistent with detection of excess Co^{I} that can reach the ring electrode at the lower nitrate concentrations. These ring–disk experiments, which promise to provide considerable insight into the mechanism of the $Co^{III/II/I}$(cyclam) electrocatalysts, are continuing.

Discussion

These results allow some conclusions to be made on the mode of action for the Co(cyclam)-electrocatalyzed reduction of nitrate and nitrite. First, the Co(cyclam) complex is an effective catalyst in strong base, approximately to the same extent as in neutral or nonaqueous solutions. Nearly complete reduction of nitrate and nitrite to mixtures of hydroxylamine and ammonia takes place with reasonable current efficiencies at a variety of electrode materials.

Scheme I

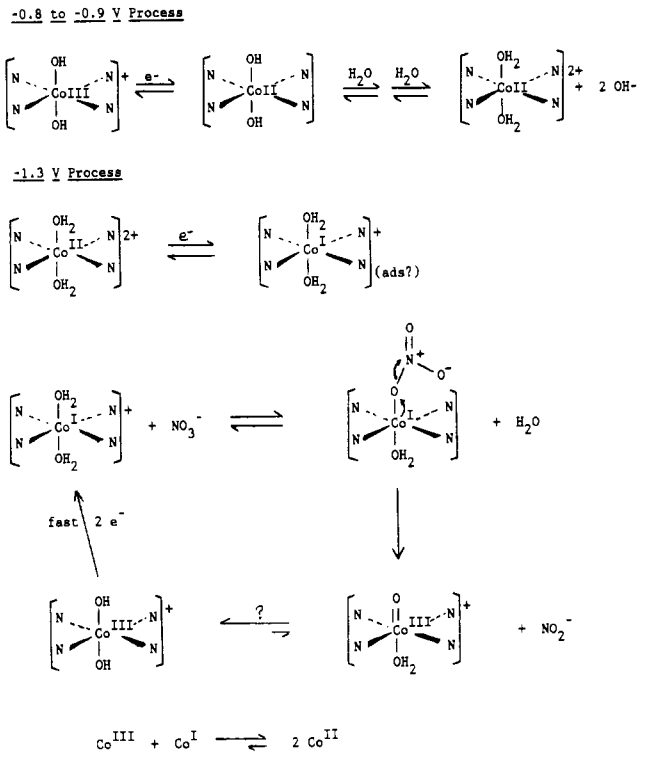

Since the $Co^{III/II}$(cyclam) wave is not significantly affected by the addition of nitrate, a key mechanistic role for a Co(I) species is indicated in agreement with a variety of other studies in which electrocatalysis by reduced cobalt macrocyclic species has been observed. A plausible mechanistic pathway that entails a two-electron reduction of a coordinated nitrate ion is proposed in Scheme I.

Several aspects of Scheme I deserve comment. First, this mechanism does not address the complete reduction of nitrate or nitrite to hydroxylamine (or other products); only the initial reductive cleavage of a nitrogen–oxygen bond is considered. In this process, no protonations or hydride transfer reactions are suggested to occur. This is consistent with the lack of dependence of the peak voltammograms of the nitrate reduction process on either the solution pH or the use of $NaOD/D_2O$ in place of H_2O.

Complexation of nitrate (or nitrite) by the Co^I species is suggested in Scheme I. This has precedent in the detection, by Gangi and Durand, of a carbon dioxide–cobalt(I) complex with a related macrocyclic amine ligand that is stable on the cyclic voltammetric time scale.[18] The magnitude of the formation constant reported by these authors is sufficient to account for the shift of the $Co^{II/I}$ wave out of the discharge region. It is interesting to note that electrocatalysis of carbon dioxide reduction by cobalt macrocyclic amines occurs in a potential region close to where the reduction of nitrate occurs and may proceed by a similar mechanism. The possibility that the key Co^I intermediate is adsorbed on the working electrode is suggested in Scheme I. A role for the electrode material is indicated by dependence of the catalytic current on the Co^{III}(cyclam) complex concentration, which differs for the various electrodes employed; see Figure 6. If the catalytic process involves only homgeneous reactions in the diffusion layer, without double-layer effects, a similar concentration dependence would be seen for different electrode materials.

In summary, Scheme I accounts for the reductive cleavage of a N–O bond in nitrate or nitrite ions in base and partially explains the electrocatalysis by Co(cyclam) ions in these systems. The catalytic action is provided by formation of an oxocobalt bond via reduction of a coordinated nitrate ion. While Scheme I is attractive, it should be stated that it is incomplete with regard to even the nature of the intermediates en route to hydroxylamine and ammonia.

Acknowledgment. This work was supported by a contract from E. I. du Pont de Nemours & Co., Inc., Savannah River Plant, Aiken, SC. Helpful discussions with Drs. S. W. Feldberg, C. E. Barnes, and S. Canagaratna are acknowledged. Drs. Mamantov and Orchard are gratefully thanked for the use of their rotating disk instrumentation.

Registry No. [*trans*-Cl_2Co^{III}(cyclam)]Cl, 15220-74-2; [*trans*-Cl_2Co^{III}(cyclam)]$^+$, 19973-61-6; [*trans*-$(OH)_2Co^{III}$(cyclam)]$^+$, 64044-37-7; [*trans*-$(H_2O)_2Co^{III}$(cyclam)]$^{3+}$, 46750-08-7; Pb, 7439-92-1; Au, 7440-57-5; Ag, 7440-22-4; Hg, 7439-97-6; NaOH, 1310-73-2; NO_3^-, 14797-55-8; NO_2^-, 14797-65-0; NH_3, 7664-41-7; NH_2OH, 7803-49-8.

(18) Gangi, D. A.; Durand, R. R., Jr. *J. Chem. Soc., Chem. Commun.* **1986**, 697-699.

Contribution from the Department of Chemistry, University of California, Santa Cruz, California 95064

Solvent Effects on the Long-Axis Intraligand Transition of $Ru(bpy)_3^{2+}$ and Related Compounds

Steven J. Milder

Received May 5, 1988

The effect of solvent polarizability on the energy of the intraligand, long-axis-polarized $\pi\pi^*$ transition of bpy in $Ru(bpy)_3^{2+}$, $Ni(bpy)_3^{2+}$, $Ru(bpy)_2Cl_2$, $Ru(bpy)_2(CN)_2$, and bpy free in solution and the ^1L_a transition of anthracene is presented. The energy at the λ_{max} value of the transition shifts as a linear function of the polarizability, $(1 - n^2)/(2n^2 + 1)$, and the slopes of the plots range between 5.6×10^3 and 13.9×10^3 cm^{-1}. INDO/S CI calculations of the singlet spectra of bpy in the cis and trans conformations are presented. It is shown that a previously reported interpretation of the effect of solvent on the energy of the visible singlet metal-to-ligand charge-transfer (^{1}MLCT) absorptions of $Ru(bpy)_3^{2+}$ is flawed. The current results support previously reported polarized absorption and emission studies, which show that throughout most of the visible ^{1}MLCT absorption band of $Ru(bpy)_3^{2+}$ the initially produced excited state is delocalized over all three ligands.

Introduction

The properties of the excited states of $Ru(bpy)_3^{2+}$ (bpy = 2,2′-bipyridine) have been extensively studied. In particular, much effort has gone into understanding the nature of the long-lived (τ = 640 ns, H_2O, 20 °C) emissive excited state.[1] A preponderance of evidence from a number of techniques shows that in fluid solution this metal-to-ligand charge-transfer (MLCT) triplet state has the transferred electron localized on one bpy at a time.[2-7]

(1) Van Houten, J.; Watts, R. J. *J. Am. Chem. Soc.* **1976**, *98*, 4853.

(2) Creutz, C.; Chou, M.; Netzel, T. L.; Okumura, M.; Sutin, N. *J. Am. Chem. Soc.* **1980**, *102*, 1309.

(3) Braterman, P. S.; Harriman, A.; Heath, G. A.; Yellowless, L. J. *J. Chem. Soc., Dalton Trans.* **1983**, 1801.

0020-1669/89/1328-0868$01.50/0 © 1989 American Chemical Society